DRD Line No. SE-5

DOE/JPL 955688-80/1

JPL NO. 9950-598

Distribution Category UC-63

DEVELOPMENT OF AN ALL-METAL THICK FILM COST EFFECTIVE METALLIZATION SYSTEM FOR SOLAR CELLS

BERND ROSS

BERND ROSS ASSOCIATES
2154 Blackmore Ct.
San Diego, CA 92109

QUARTERLY REPORT NO. 1
MAY 1980 - JULY 1980

AUGUST 1980

Contractual Acknowledgement

The JPL Low-Cost Silicon Solar Array Project is sponsored by the U.S. Department of Energy and forms part of the Solar Photovoltaic Conversion Program to initiate a major effort toward the development of low-cost solar arrays. This work was performed for the Jet Propulsion Laboratory, California Institute of Technology by agreement between NASA and DOE.

DRD Line No. SE-5

DOE/JPL-955688-80/4
Distribution Category UC-63

DEVELOPMENT OF AN ALL-METAL THICK FILM COST EFFECTIVE METALLIZATION SYSTEM FOR SOLAR CELLS

BERND ROSS

BERND ROSS ASSOCIATES
2154 Blackmore Ct.
San Diego, CA 92109

QUARTERLY REPORT NO. 1
MAY 1980 - JULY 1980

AUGUST 1980

Contractual Acknowledgement

The JPL Low-Cost Silicon Solar Array Project is sponsored by the U.S. Department of Energy and forms part of the Solar Photovoltaic Conversion Program to initiate a major effort toward the development of low-cost solar arrays. This work was performed for the Jet Propulsion Laboratory, California Institute of Technology by agreement between NASA and DOE.

TABLE OF CONTENTS

LIST OF FIGURES

LIST OF TABLES

1.0 Summary

Materials including copper powders, silver-fluoride and silicon wafers were procured.

Copper pastes were prepared by the subcontractor. Properties of the recent pastes did not reproduce earlier results in rheology and metallurgy. Electrodes made with pastes produced under the previous contract were analyzed and compared with the raw materials.

A needle-like structure was observed on the earlier electroded solar cells, and was identified as eutectic copper-silicon by electron probe Xray spectroscopy. The existence of this phase was thought to benefit electrical and metallurgical properties of the contact. Subsequently electrodes made from new material were also shown to contain this phase while simultaneously having poor adhesion.

A front contact paste was formulated.

A solar cell experiment is in process.

2.0 Introduction

The purpose of this study is to provide economical, improved thick film solar cell contacts for the high-volume production of low-cost silicon solar array modules for the LSA Project.

This work is based upon the concept of an all metal screenable electrode ink, investigated in Contract #955164. It was first found that silver powder with lead acting as a liquid sintering medium and with silver fluoride acting as an oxide scavenger, continuous, adherent electrode layers result on silicon. During the final phase of the antecedent contract it was shown that base metals such as copper can likewise be sintered to provide an ohmic contact on silicon when appropriately doped. The most successful screened solar cell contacts were achieved using germanium-aluminum and silicon-aluminum eutectics as additions to the pastes for back contacts.

The objectives of the investigation are to provide all metal screenable pastes using economical base metals, suitable for application to low-to-high conductivity silicon of either conductivity type and possibly to aluminum surfaces.

3.0 Analysis of Successful Copper Pastes and Substrates

3.1 Microscopic Examination and Optical Microscopy

Solar cells screened with S079 doped with silicon-aluminum eutectic and with S080 doped with germanium-aluminum eutectic (back-contacts only) and fired at 550°C with the two step firing process had good IV characteristics and efficiencies as previously reported.[1,2] Portions of cells with both electrode pastes were cleaved and the cross sections examined with optical and SEM micrography. The micrographs exhibit a remarkable lion tooth shaped growth structure based upon the solar cell silicon substrate and extending throughout the copper grain matrix.

This can be seen in Figures 1, 2 and 3 which are black and white reproductions of color photographs taken at a magnification of 200X through an optical microscope. Figure 1 shows a portion of the cleaved cross section of an electrode screened with S079 (containing aluminum-silicon eutectic), and Figures 2 and 3 similarly depict S080, the paste with the aluminum-germanium eutectic. While it is not possible to show this in a report of this type, the color of the structures clearly shows them to be of a nature different from the copper grain matrix. A color comparison shows the spike-like structures to be similar to the substrates. One might be led to believe, that melting or penetration into the silicon substrate has occurred by virtue of the structure of the cleave facets just below the spikes. However, this can be better explained by the mechanical nature of the

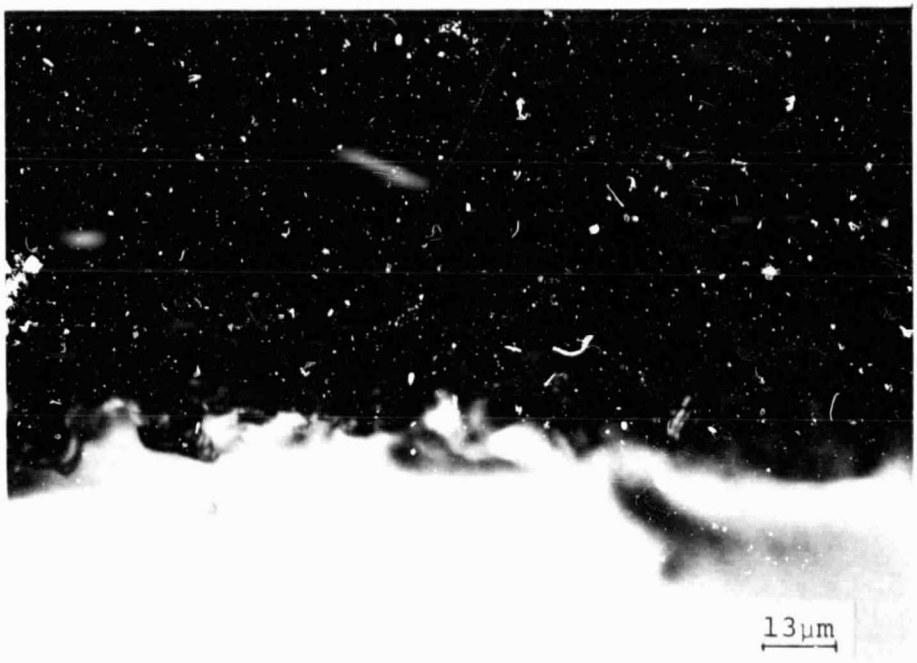

Figure 1. Enlarged optical photomicrograph of cross section of S079 electrode on solar cell. Magnification 200X, optical enlargement 8.25X. (Black and white reproduction of color photograph).

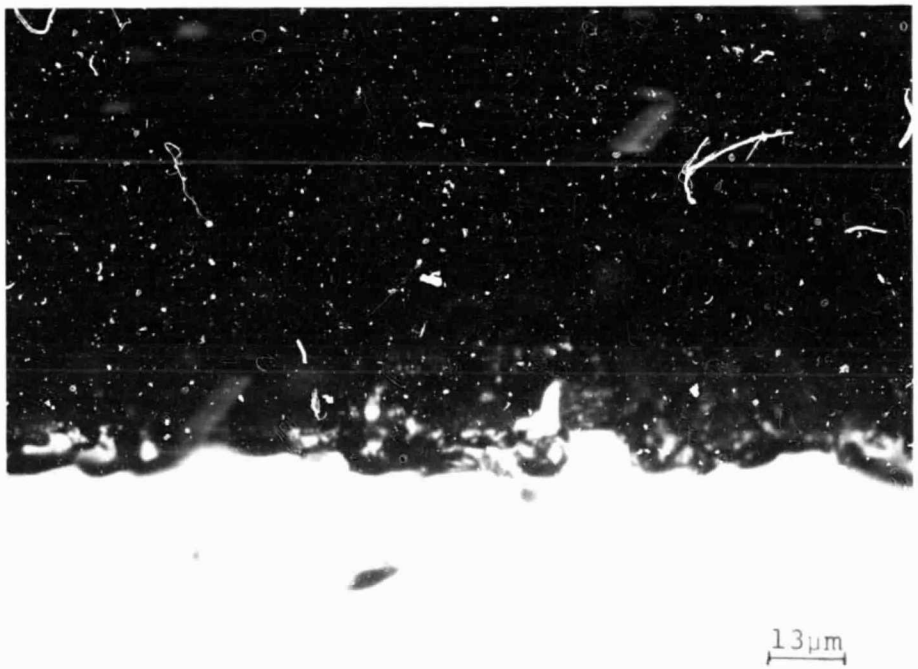

Figure 2. Similar to Figure 1 of S080 cross section.

Figure 3. Optical micrograph of S080 paste approximately 85 wt. % copper, 5 wt. % silver fluoride, 5 wt. % germanium-aluminum eutectic, 5 wt. % lead. Combined optical and photographic enlargement about 1600x.
Color of spikes suggests semiconductor material.

cleaving action, which dictates that the crack circumnavigates those portions of the wafer which are stronger (thicker). The optical photographs were taken at the relatively low magnification to reduce the depth of field problem (still quite evident), and were subsequently enlarged photographically. A measure of dimensions and proportionality is still maintained by remembering that the average thickness of the copper electrode is approximately 0.5 mil or 13 μm. There does not appear to be a significant difference between the electrodes made from S079 or S080.

SEM photography was undertaken in order to obtain clearer images at high magnification free from the depth of field focussing problem and to allow compositional analysis of the lion tooth structures by Xray fluorescence analysis.

Figure 4 shows a view of the sintered surface of S080 paste at 2000X magnification. The lion tooth structures are not readily identifiable in this view. However, one of the early SEM photomicrographs taken during previous investigations[3] suggests the presence of such features (see Figure 5 left side of photograph 1/3 down from the top).

Figure 6 is another view of the cross section of paste S080 at 580X magnification. Note the previously mentioned cleavage structure below the silicon surface. Figure 7 and 8 show higher magnifications of the same region. Figures 9 and 10 of another region show that the spikes do not all incline in the same direction. Figure 10 shows detail of a spike at

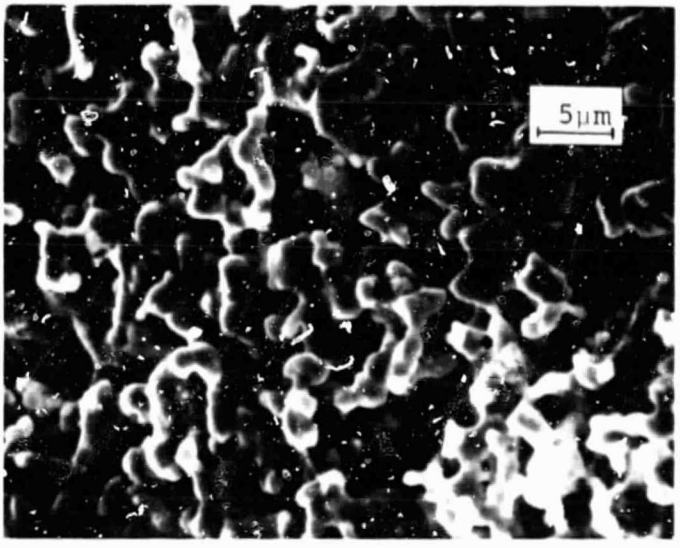

Figure 4. SEM micrograph of surface of sintered SO80 electrode fired at 550°C (magnification 2000X).

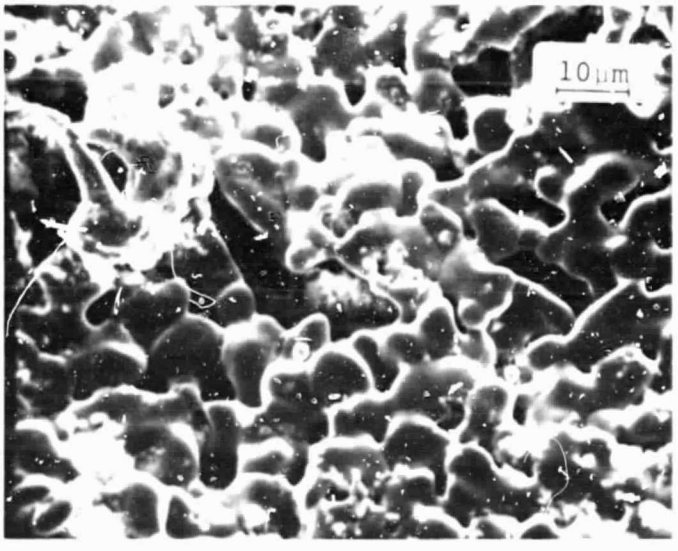

Figure 5. SEM photo micrograph of surface of sintered SO80 electrode fired at 700°C (magnification 975X).

Figure 6.
580X

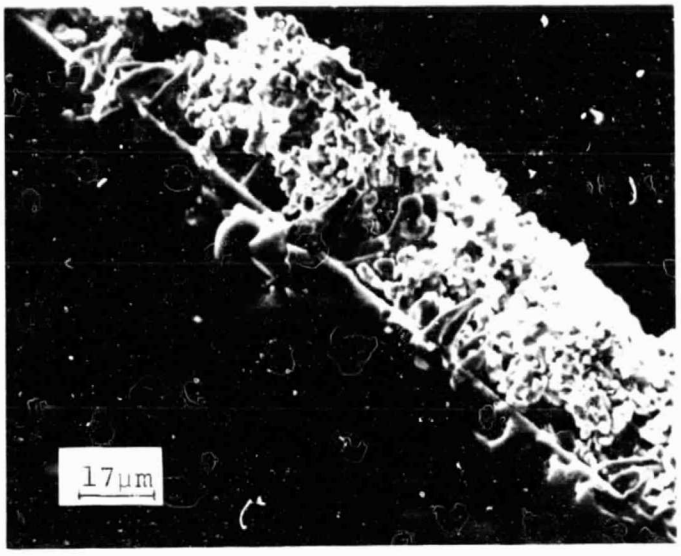

Figure 7.
1150X

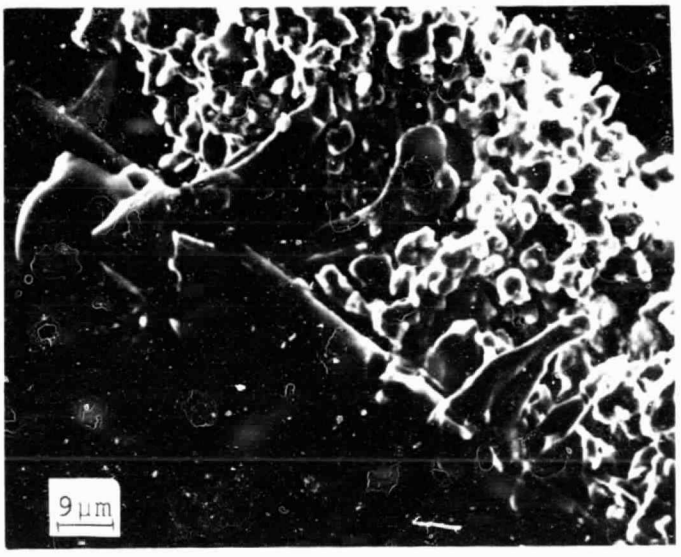

Figure 8.
2300X

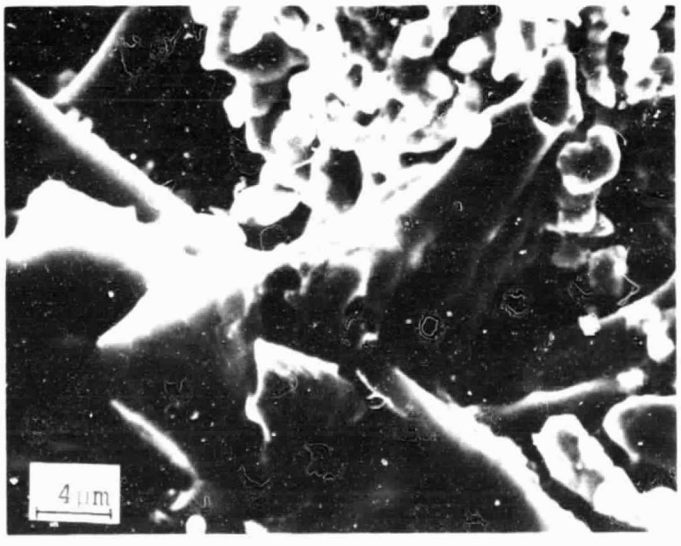

Cross Sectional SEM micrographs of S080 electrodes fired at 550°C at indicated magnifications.

Figure 9.
910X

Figure 10
4600X

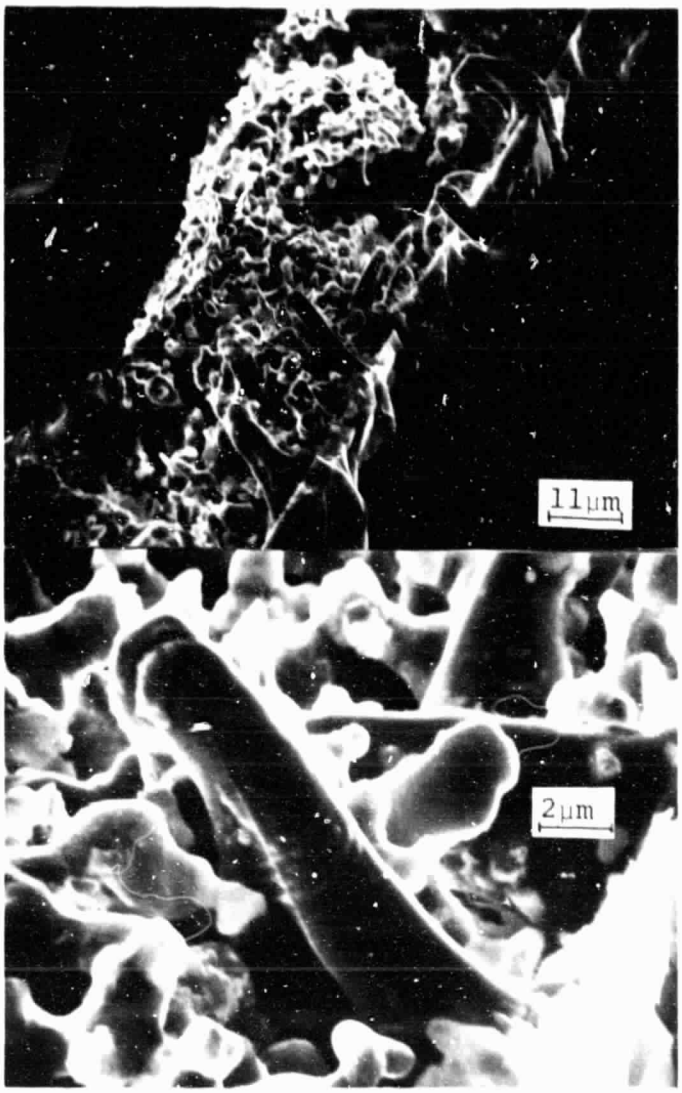

SEM micrograph of cross section of SO80 electrode fired at 550°C at indicated magnifications.

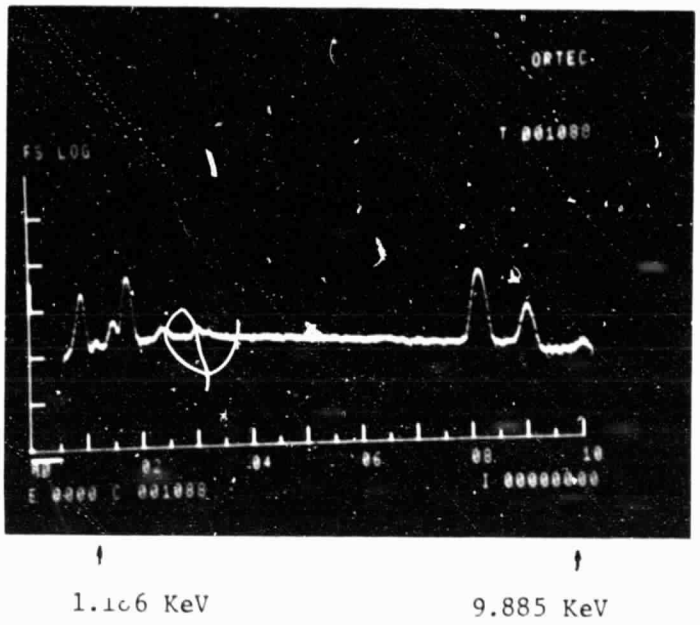

Figure 11. Xray fluorescence spectral scan of S080 fired electrode cross section. Indicated peaks are GeL_{α_1} and Ge K_{α_1} lines.

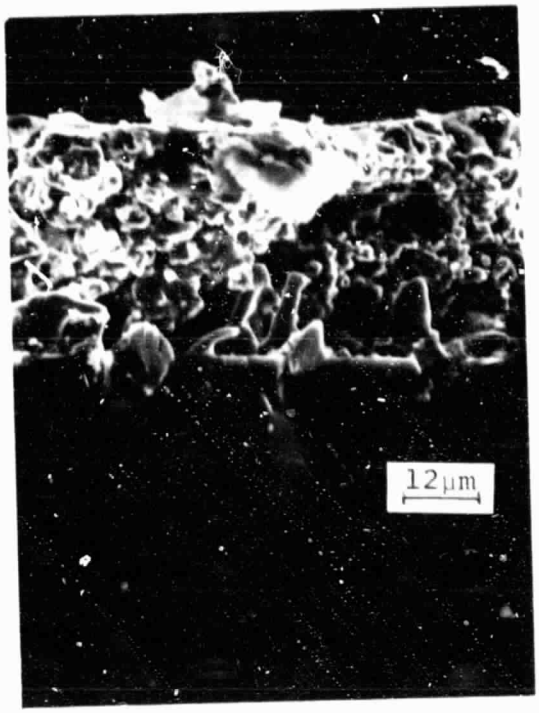

Figure 12 870x

Figure 13 4400x

Cross section of S079 electrodes fired at 550°C

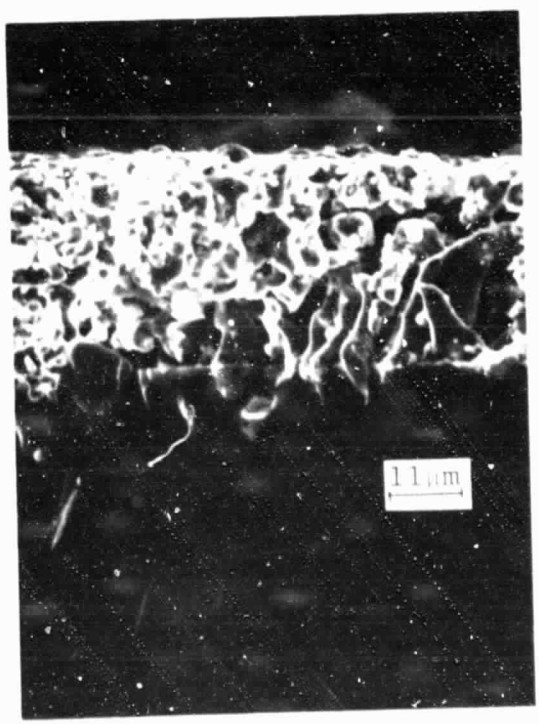

Figure 14 890x

Figure 15 4400x

Similar to Figure 12 and 13 above. Note subsurface structure.

relatively high magnification (4600X). Figure 11 is the spectral scan resulting from Xray fluorescence analysis. The germanium $L\alpha_1$ line at 1.186 KeV and $K\alpha_1$ at 9.885 KeV are indicated. While the germanium was significant in a general scan (as shown), it could not be detected when an attempt was made to focus upon the spike structure.

SEM photo micrographs of sections of S079 are shown in the next set of illustrations Figure 12 and 13 at magnifications 870X and 4400X respectively are similar to the structures observed with S080. In Figures 14 and 15, at 890X and 4400X respectively, the sub surface facetting is particularly evident, presumably because of the massive grown superstructure.

4.0 Analysis of Recent Batches of Copper Paste, Electrodes And Substrates

Test patterns and some solid electrodes were printed on polished wafers with pastes S071 and S079. Six different batches of S071 were fired in this experiment. A portion of these test samples were fired in the AVX laboratory belt furnace in forming gas (N_2 + 5% H_2), the remainder in the two-step firing process, in the quartz tube furnace, all at 550°C. Results from this experiment were mixed in appearance and in adhesion, with belt furnace fired samples showing poorer adhesion and a more oxidized appearance. A specimen with silver fluoride made by Apache Chemical Company gave extremely poor adhesion. Further, it was noted that the paste surface darkened significantly in a few days, which had not been noted previously. In order to determine whether starting materials were similar to previous lots, analytical tests were run, including emission spectroscopy on silver fluoride, as well as thermal gravimetric analysis (TGA) and differential thermal analysis (DTA).

Results of the analyses are shown in Appendix 1, 2 and 3. No significant variations were seen.

Paste fabrication parameters were examined, including fineness of grind (FOG) and powder surface area. Again, no causal deviations were noted.

SEM micrography was performed on powders, as well as fired electrodes. Copper powder grains were generally similar to previous batches, although some grain aggregations were seen.

4.0 Cont.

Figure 16 shows a sequence of SEM photomicrographs taken of S071 fired at 600°C in forming gas (nitrogen 90% hydrogen 10%) at various magnifications. The spike formation is clearly in evidence. While the spike growth phase was originally hypothesized to be a regrowth material resulting from a silicon or germanium rich eutectic aluminum solution, precipitating the semiconductor phase during cooling, and thusly providing a high conductivity p-type surface for attachment of the copper grains.[4] Since excellent ohmic contacts had been obtained, it was thought the hypothesis was corroberated. Furthermore, the good characteristics of solar cells obtained previously [1] led some workers to suggest that a diffusion barrier must exist between the silicon base material and the copper electrode. This was proposed because the firing step of the screened electrode is quite sufficient to cause copper to diffuse to the p n junction, assuming the published diffusion coefficient of copper and silicon.[6]

It was therefore surprising to observe the spike structure in paste material that does not contain silicon or germanium-aluminum eutectic additions.

A further unexpected attribute of the electrodes made with the new materials was poor adherence despite the spike formation.

Figure 17 shows an SEM photomicrograph of an electrode fragment in the act of separating from the substrate at two indicated magnifications. It can be seen that the spike formation

4.0 Cont.

is in evidence, and has in fact remained a part of the substrate, while the sintered copper layer has been disengaged from the dovetailed structure. It became of major interest to analyze the nature and composition of the spike.

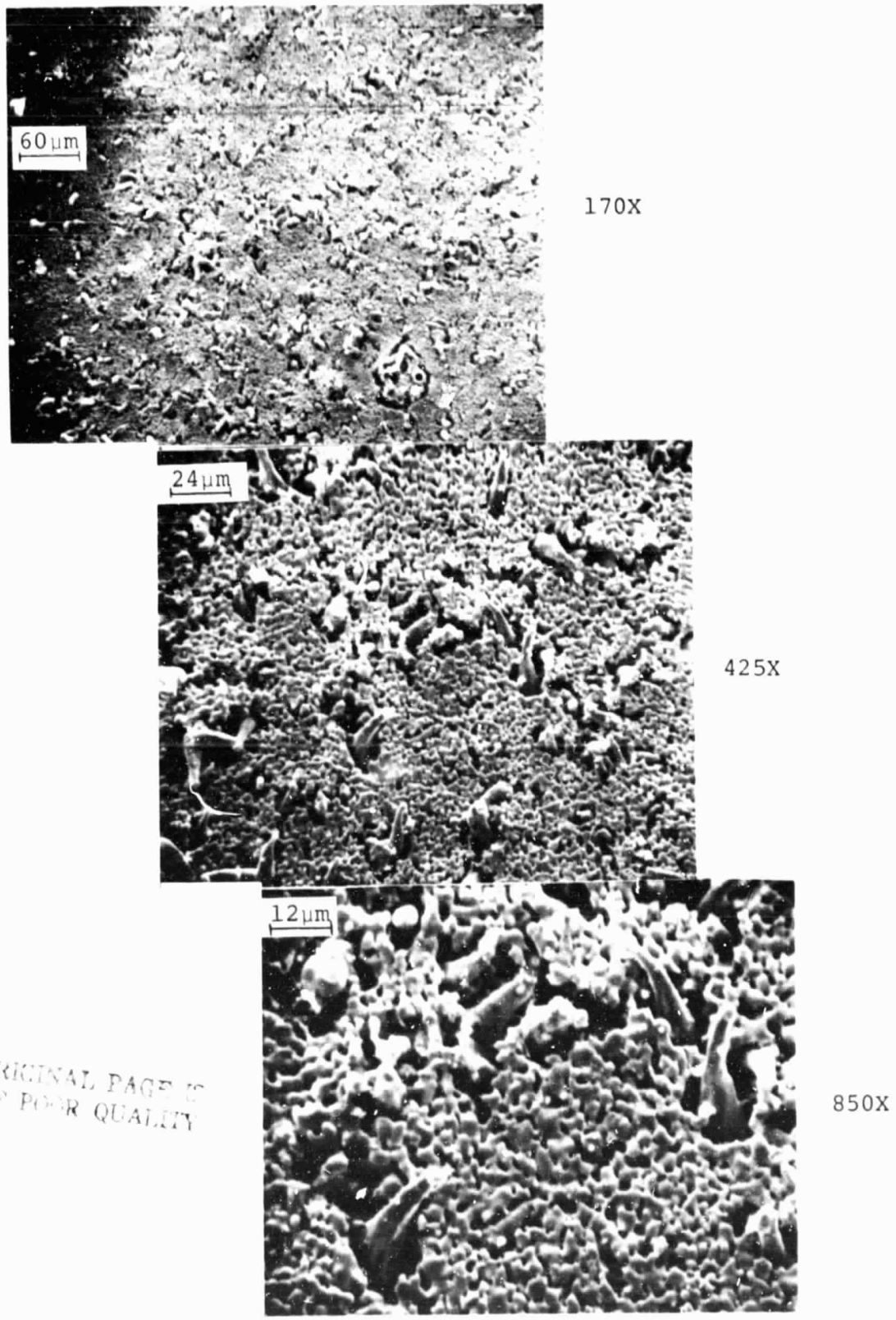

Figure 16. Sequence of photomicrographs of S071-A9, fired at 600°C in forming gas

450X 825X

Figure 17. S071 Electrode partially pulled from substrate (in cross section)

5.0 Electron Microprobe Analysis

Several attempts were made to obtain dispersive Xray spectra in the Cambridge SEM of the spike structure only. This effort was unsuccessful. It was therefore decided to utilize the CAMECA electron microprobe for this purpose. No difficulty was experienced during this analysis. Figure 18 shows the structure that was analyzed by the electron probe, taken in situ. The electron beam was centered on the spike slightly to the left of the center of the photomicrograph.

Table 1 gives the composition determined from the analysis. The column headed "General" gives compositional data for the total electrode matrix cross section.

Comparing this data to the phase diagram (Figure 19) for the copper silicon system, shows the 29.80 at% value to coincide with the eutectic line of copper-silicon. The melting point for the eutectic is given as 802^{o}C which is considerably above the 550^{o}C firing temperatures normally employed. However it is obvious from the Table that we are not dealing with a pure alloy. Whether the other constituents (aluminum, silver and lead) suffice to depress the melting point to that degree (250^{o}C) is presently not known.

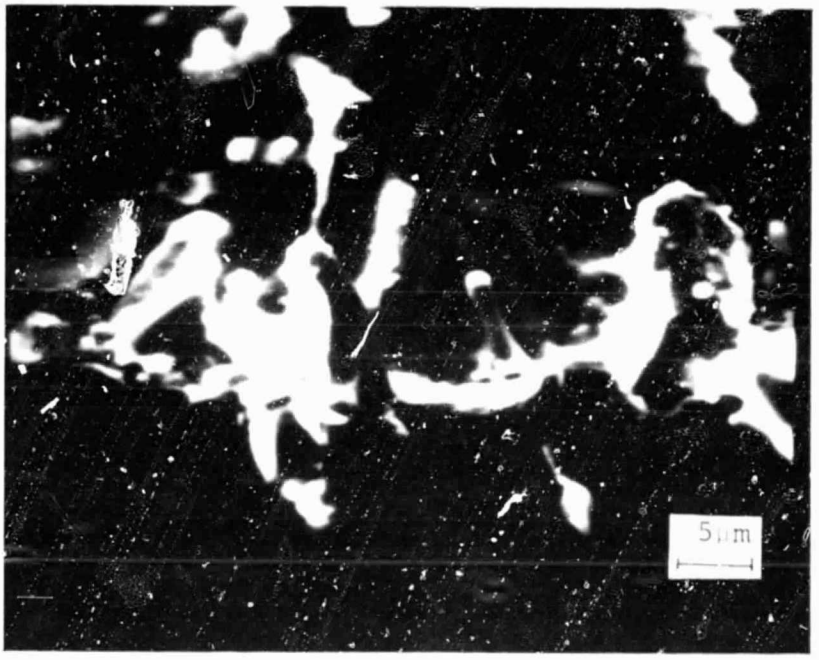

Figure 18. Electron microprobe analysis (CAMECA microprobe) of spike structure; target structure photographed in CAMEBAX at 2000x, paste S079

TABLE 1

Composition According to Microprobe

Silver	0.38 at %	0.84 at %
Copper	63.45	81.08
Silicon	29.80	3.79
Lead	0.17	6.76
Aluminum	1.20	7.54

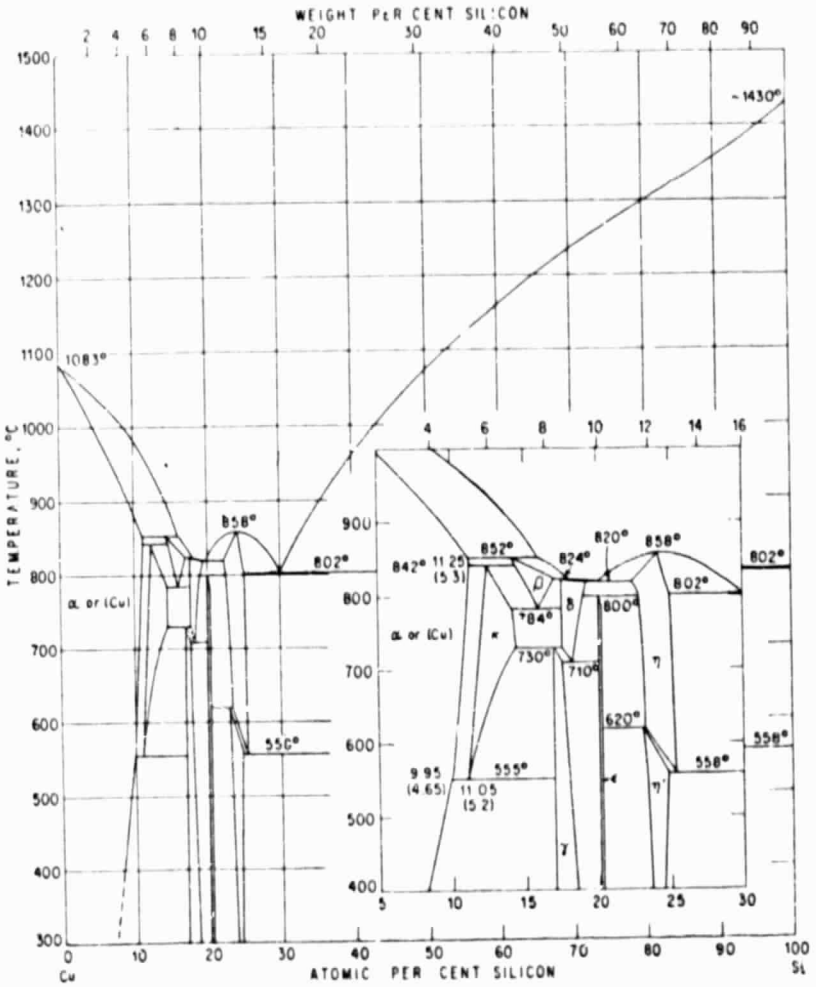

Figure 19. Phase diagram of copper-silicon system[5]

6.0 Solar Cell Experiments

Cells containing phosphorous diffused layers with various junction depths and with silicon oxide chemical vapor deposition (CVD) coatings on the front surface were received from ASEC. Since a large number of samples were required for the planned experiment, cells were cleaved into quarters using a tungsten carbide point, impacting the wafer near the center. While this method had worked well in the past, a relatively large number of specimen cleaved unevenly or even shattered. Also, the rheological properties of the previous pastes could not be reproduced. Pastes were highly thixotropic, yielding prints of questionable quality with a surface topography reproducing the wire mesh. In view of these problems, it was decided to postpone the cell experiments until larger quantities of wafers were available for this experiment, and better flow properties could be obtained with the pastes.

For front contact experimentation an electrically neutral paste (without intentional dopant) and an n-type doped paste were prepared. Details of the considerations for front contact electrodes and other concerns for the solar cell experiment will be furnished in the next quarterly report.

8.0 Conclusions and Problems

A major conclusion reached in this quarter is the existence of a silicon-copper eutectic phase in the form of the spike structure, occurring regardless of eutectic additions to pastes, and apparently not a factor in paste adhesion. This also allows the further observation that the diffusion rate of copper in undiffused silicon is likely to be considerably lower than previously estimated, leading to the hypothesis that the anomalous copper diffusion along the dislocation array in the front layer of the junction is responsible for previously observed degradation effects associated with copper junction shunting.

A major problem is the inability to reproduce earlier results, particularily inadequate adherence of copper electrodes.

9.0 Plans and Recommendations

Further analyses will be undertaken to attempt to define the differences between the original successful pastes and materials having poor adherence.

Variations of paste materials sources will also be tried.

The solar cell experiment will be completed, including efforts with pastes designed specifically for front contacts.

9.0 Appendix

1a Differential gravimetric analysis of silver fluoride

b Differential thermal analysis of silver fluoride

2. Atomic absorption spectral analysis report on silver fluoride

3. Qualitative analysis report on silver fluoride

PART NO. 990092

RUN NO. ___ DATE 5/21/82 OPERATOR Scott Billetdo SAMPLE ATM N_2 @ ___ FLOW RATE 2-3 SCFH	T-AXIS SCALE, mv/in 0.8 PROG. RATE, °C/min ___ HEAT ___ COOL ___ ISO ___ SHIFT, in 0	DTA-DSC SCALE, °C/in ___ (mcal/sec)/in ___ WEIGHT, mg 40 mg REFERENCE Al_2O_3 20 uv 5MV/IN	TGA SCALE, mg/in 5mg/IN SUPPRESSION, mg ___ WEIGHT, mg 35 Mg TIME CONST., sec ___ dY, (mg/min)/in ___	TMA SCALE, mils/in ___ MODE ___ SAMPLE SIZE ___ LOAD, g ___ dY, (10X), (mils/min)/in ___	A_gF (Alla #10125) #1 (Alla)

A1 Thermal Gravimetric Analyses and Differential Thermal Analyses of Silver Fluoride

a

b

m.p. 435°C

2.4 mg loss of H_2O

$\frac{95-2.4}{135} = 93.14\%$ residue

MEASURED VARIABLE ___

0 100 200 300 400 500 600 700 800 900 1000 1100

TEMPERATURE, °C (Pt/Pt-13% Rh)

26

Date 4/9/80

Requested By Scott Billets

Type of Material AgF

Lot # 030579

Analysis Requested: AA
(sodium content)

Specific Instructions or Precautionary Measures:
: Moisture sensitive compound

RESULTS: (Unless otherwise attached)

#1 37 ppm Na

#2 38 ppm Na R Braun 4/9/80

ANALYTICAL CHEMISTRY REQUEST FORM

Date 3/11/80

Requested By Scott Billets

Type of Material Silver fluoride (AgF) #1 & #2

Lot # 030579

Analysis Requested:

Qualitative (determine if contaminants are present)

Specific Instructions or Precautionary Measures:

Must be kept in dessicator (moisture sensitive)

RESULTS: (Unless otherwise attached)

#1 - Pb (very faint)
Mg
Si
Fe
Al
Cu
Na
Ca

#2 - Mg
Si
Fe
Al
Cu
Na
Ca

JW Morgan 3-11-80

10.0 References

1. B. Ross, Proceedings of the 14th IEEE Photovoltaic Specialists Conference, San Diego, CA, page 787 (1980)

2. B. Ross, Proceedings of the 14th IEEE Photovoltaic Specialists Conference, San Diego, CA, page 1406 (1980)

3. B. Ross, Extension Final Report, Development of Economical Improved Thick Film Solar Cell Contacts, DOE/JPL 955164-79/4 (Dec 1979)

4. B. Ross, Proceedings of the 14th IEEE Photovoltaic Specialists Conference, San Diego, CA, page 1406 (1980)

5. M. Hansen and K. Anderko, "Constitution of Binary Alloys" McGraw-Hill, page 631 (1958)

6. M. G. Coleman, R. A. Pryor and T. G. Sparks, Quarterly Technical Report #4, Automated Array Assembly Task, DOE/JPL 954847-79/5, page 18 (1979)

11.0 Progress on Program Plan

PROGRAM ACTIVITY	MONTHS AFTER AWARD												
	1	2	3	4	5	6	7	8	9	10	11	12	13
Cu Metallization (A)	▽	———		△									
Metallization (B)			▽			△							
Metallization (C)					▽				△				
Metallization (D)							▽				△		
Analysis and Test	▽	———										△	
Cell Delivery											.		
Cost Analysis - SAMICS											.		
Reports - Monthly		X		X		.	.			.		.	
- Quarterly				X			.			.			
- Final												.	
Review Meetings			.		.		.		.			.	.
Project Integration Meetings	.					.				.			
Project Workshops	As Specified by JPL												

▽ Start

△ Complete

. Proposed

X Completed